SCIENCE CHINA
Life Sciences

• RESEARCH PAPER •

June 2013 Vol.56 No.6: 571–580
doi: 10.1007/s11427-013-4489-x

Activities of principal photosynthetic enzymes in green macroalga *Ulva linza*: functional implication of C_4 pathway in CO_2 assimilation

XU JianFang[1], ZHANG XiaoWen[2], YE NaiHao[2*], ZHENG Zhou[1], MOU ShanLi[2], DONG MeiTao[3], XU Dong[2] & MIAO JinLai[1*]

[1]*Key Laboratory of Marine Bioactive Substance, The First Institute of Oceanography, State Oceanic Administration, Qingdao 266061, China;*
[2]*Yellow Sea Fisheries Research Institute, Chinese Academy of Fishery Sciences, Qingdao 266071, China;*
[3]*Qingdao Agricultural University, Qingdao 266109, China*

Received September 18, 2012; accepted April 19, 2013

The green-tide-forming macroalga *Ulva linza* was profiled by transcriptome sequencing to ascertain whether the alga carries both C_3 and C_4 photosynthesis genes. The key enzymes involved in C_4 metabolism including pyruvate orthophosphate dikinase (PPDK), phosphoenolpyruvate carboxylase (PEPC), and phosphoenolpyruvate carboxykinase (PCK) were found. When measured under normal and different stress conditions, expression of *rbc*L was higher under normal conditions and lower under the adverse conditions, whereas that of PPDK was higher under some adverse conditions, namely desiccation, high salinity, and low salinity. Both ribulose-1, 5-biphosphate carboxylase (RuBPCase) and PPDK were found to play a role in carbon fixation, with significantly higher PPDK activity across the stress conditions. These results suggest that elevated PPDK activity alters carbon metabolism in *U. linza* leading to partial operation of the C_4 carbon metabolism, a pathway that, under stress conditions, probably contributes to the hardy character of *U. linza* and thus to its wide distribution.

C_4 pathway, PPDK, RuBPCase, *Ulva linza*

Citation: Xu J F, Zhang X W, Ye N H, et al. Activities of principal photosynthetic enzymes in green macroalga *Ulva linza*: functional implication of C_4 pathway in CO_2 assimilation. Sci China Life Sci, 2013, 56: 571−580, doi: 10.1007/s11427-013-4489-x

Plants can be classified into three major categories—C_3 plants, C_4 plants, and Crassulacean acid metabolism (CAM) plants—based on the mechanism by which they assimilate carbon during photosynthesis. The most common and the most primitive of the three photosynthetic pathways is the C_3 pathway, which is characterized by an initial CO_2 carboxylation to form a 3-carbon acid, namely phosphoglyceric acid (PGA) [1]. However, atmospheric CO_2 is first incorporated into C_4 acids in C_4 pathway. The C_4 pathway is a complex trait that has evolved from ancestral C_3 plants via a series of anatomical and physiological adaptations [2,3]. Compared with C_3 plants, C_4 plants utilize a biochemical CO_2-concentrating mechanism combining a faster rubisco that make them to use nitrogen and water more effectively [4]. C_3-C_4 intermediates which possess the characteristics of both C_3 plants and C_4 plants, may be a transitional stage in the evolution of C_4 pathway from C_3 pathway [5].

The mechanisms of uptake and fixation of inorganic carbon (Ci) have been researched extensively in land plants whereas information on the photosynthetic pathway in aquatic plants is relatively scarce, and no fixed standard is so far available for classifying them on the basis of their photosynthesis pathway. Aquatic higher plants, such as some species of *Hydrilla*, *Egeria*, *Orcuttia*, and *Eleocharis*,

*Corresponding author (email: yenh@ysfri.ac.cn; miaojinlai@163.com)

can utilize a C_4 photosynthetic system that surprisingly lacks the Kranz dual-cell compartmentation found in most terrestrial C_4 plants [6]. Under some forms of stress, malate decarboxylation by NADP malic enzyme (NADP-ME) in the chloroplasts of such facultative C_4 species triggers a chloroplastic CO_2 concentrating mechanism (CCM) [6]. Both C_4 and C_3 cycles operate in the same cell, with phosphoenolpyruvate carboxylase (PEPC) and ribulose bisphosphate carboxylase-oxygenase (rubisco) being sequestered in the cytosol and chloroplasts respectively [6]. *Hydrilla verticillata*, an aquatic plant which typically exhibits C_3 gas-exchange and biochemical characteristics, can be induced to be a C_4-based CCM under exposure to low CO_2 within 10–12 days [7]. The change from C_3 to C_4 can occur without the production of new leaves, and has been documented *in situ* (in lakes) as well as the laboratory [7,8]. Under low CO_2 concentration, C_4 pathway genes are up-regulated and expressed in the original C_3 mesophyll cell [7,9].

Marine algae, despite CO_2-limiting conditions in the oceans [10], manage to increase the steady-state CO_2 concentration around rubisco, the principal photosynthetic carboxylase, by actively using CCM [11–13]. This mechanism diminishes the wasteful process of photorespiration by increasing the ratio of CO_2 to O_2. Despite its great ecological impact, photosynthetic carbon acquisition by marine algae is only poorly understood so far. Photosynthetic carbon fixation pathways of marine macroalgae generally follow the C_3 pathway [14], however, recent metabolic labeling and genome sequencing data suggest that the algae also use the C_4 pathway, and the marine diatom *Thalassiosira weissflogii* has been reported to do so in a single cell [15,16]. The relevant genes involved in C_4 photosynthesis were also observed in the diatom *Phaeodactylum tricornutum* [17] and the green alga *Ostreococcus tauri* [18]. PEPC activity in *T. weissflogii* increases in cells acclimatized to low CO_2, indicating a probable link between inorganic carbon uptake and PEPC [15]. McGinn and Morel (2008) also observed two PEPC gene transcripts in *T. pseudonana* cells up-regulated 2- to 4-fold in order to acclimatized to low CO_2 [19]. When the activity of PEPCase was restrained by 3,3-dichloro-2-dihydroxyphosphinoylmethyl-2-propenoate in *T. weissflogii* cells adapted to low CO_2 (10 μmol L^{-1}), the whole cell photosynthesis decreased by more than 90%, but had little influence on photosynthesis in the C_3 algae *Chlamydomonas* sp. [16].

The genus *Ulva* is believed to behave as a typical C_3 plant at the biochemical level [20]. *Ulva linza*, the dominant *Ulva* species along the coastline of the Yellow Sea before May [21], is a representative green-tide-forming macroalga [22]. Being an intertidal species, *U. linza* must face and cope with extremes of temperature, solar radiation, and desiccation by means of high physiological efficiency and molecular adjustment [23,24]. Moreover, evolution places intertidal multicellular green algae between unicellular green algae and lower land plants; the organisms represent an important link in the evolution [25] and are therefore particularly valuable in investigating the evolution of the CO_2 fixation pathway. The present study, by transcriptomic sequence and analysis, first confirmed the coexistence of genes necessary for C_3 and C_4 pathway in *U. linza* and subsequently focused on two key enzymes, namely RuBPCase and PPDK. Ribulose-1,5-biphosphate carboxylase, a key enzyme of the C_3 pathway, is widely distributed in photosynthetic organisms and catalyzes the photosynthetic fixation of CO_2 through the Calvin cycle. Pyruvate orthophosphate dikinase, a key enzyme of the C_4 pathway, catalyzes the formation of phosphoenolpyruvate (PEP), the initial acceptor of CO_2 in the C_4 pathway [26]. The formation of PEP by PPDK is considered to be the rate-limiting step for the lowest reaction rate in the C_4 pathway [27,28]. Our results lead us to believe that *U. linza* may perform C_4 photosynthetic pathway and contribute to the large-scale bloom of *U. linza*.

1 Materials and methods

1.1 Sampling and culture conditions

Samples of *U. linza* were collected in April 2011 from the intertidal zone (35°35′N, 119°30′E) of Zhanqiao Wharf, Qingdao, China. In the laboratory, the intact samples were washed several times with sterile seawater, sterilized with 1% sodium hypochlorite for 2 min, and then rinsed with autoclaved seawater. The sterilized material was then placed into an aquarium containing enriched and continually aerated seawater (500 μmol L^{-1} $NaNO_3$ and 50 μmol L^{-1} NaH_2PO_4) and maintained at 10°C under a cycle comprising 12 h of light alternating with 12 h of darkness. The light intensity was 50 μmol m^{-2} s^{-1} provided by cool-white fluorescent tubes [28].

1.2 Transcriptome sequencing

U. linza were exposed under low temperature (5°C) and high temperature (42°C) for 1 h, respectively. The samples were placed under high light intensity (1000 μmol m^{-2} s^{-1}), high salinity (93‰) and UV-B radiation (60 μW cm^{-2}) for 3 h, respectively. Total RNA from every treated sample was extracted and purified, followed by synthesis and purification of double-stranded cDNA and sequencing of cDNA using a Roche GS FLX Titanium platform. To reconstruct the metabolic pathways in *U. linza*, high-quality reads were assigned to the Kyoto Encyclopedia of Genes and Genomes (KEGG) using the software package MEGAN (version 4.0) [29].

1.3 Sequence analysis

The cDNA open reading frame (ORF) sequence of *rbc*L,

acquired from GenBank, and of *PPDK*, obtained by transcriptome sequencing, were examined for homology with other known sequences using the BLAST X program available at the website of the National Center for Biotechnology Information (www.ncbi.nlm.nih.gov/blast). The deduced amino acid sequence was analyzed with the Six Frame Translation of Sequence system (http://molbiol.ru/eng/scripts/01_13.html). At last, the *rbc*L cDNA sequence (DQ813497) of ORF was acquired from GenBank with a 1425 bp sequence, which encodes 474 amino acid residues. The *PPDK* cDNA sequence (JN222388) of ORF was obtained from the *U. linza* transcriptome database with a 2700 bp sequence encoding 889 amino acid residues.

1.4 Chlorophyll fluorescence measurements

Fluorescence of PS II of *U. linza* was determined *in vivo* by pulse amplitude modulation using Dual-PAM-100 (Walz GmbH, Germany). The minimum fluorescence yield (F_0) was determined using 15 min dark-adapted samples and the maximum fluorescence yield (F_m) obtained by applying saturating pulses [30].

The following formulae were used to calculate the optimum quantum yield (F_v/F_m) and the effective PS II quantum yield (Y(II)), which reflect the potential and the actual rate of photosynthesis, respectively [31]:

$$F_v/F_m=(F_m-F_0)/F_m,$$

$$Y(\mathrm{II})=(F'_m-F)/F'_m,$$

where F'_m represents the maximum fluorescence yield from light-adapted samples. F is the fluorescence yield from light-adapted samples.

All the results in this study were expressed as mean values, and these were used for statistical analysis (ANOVA) using SPSS (version 17.0).

1.5 Stress treatments

The alga was subjected to different kinds of stress, namely desiccation and differing levels of salinity, light intensity, and temperature. Desiccation stress took the form of exposure to 50 μmol photons m^{-2} s^{-1} for different durations (0, 1, 2, 3, 4, and 5 h); salinity stress consisted of subjecting the organism for 1 h to different salt concentrations (0‰, 15‰, 30‰, 45‰, and 60‰); and light intensity treatment consisted of 1 h exposure to 0, 50, 200, 600, 1000, and 2000 μmol m^{-2} s^{-1}. For the three forms of stress, temperature was constant at 10°C, and light intensity during the salinity treatment and the temperature treatment was maintained at 50 μmol photons m^{-2} s^{-1}. Temperature stress involved exposure for 1 h to 0, 5, 10, 15, 20, 25, and 30°C. Following each stress treatment, F_v/F_m and Y(II) was measured by Dual-PAM-100, *rbc*L and *PPDK* mRNA expression level determined using qPCR, and RuBPCase and PPDK activity assessed.

1.6 Real-time quantitative PCR

Total RNA of *U. linza* samples exposed to each form and level of stress was extracted using TRIzol reagent (Invitrogen, Carlsbad, CA, USA) as specified in the user manual and dissolved in diethypyrocarbonate (DEPC)-treated water. The cDNA used for real-time quantitative PCR was synthesized from the total RNA using Moloney murine leukemia virus reverse transcriptase (Promega Biotech Co., Madison, Wisconsin, USA).

The real-time quantitative PCR reactions were performed with the ABI StepOne Plus Real-Time PCR System (Applied Biosystems, USA) using SYBR Green fluorescence (TaKaRa) according to the manufacturer's instructions. To normalize the relative expression of the selected genes, an 18S rDNA gene was used as reference [32]. Three pairs of gene-specific primers (Table 1) were designed according to the *rbc*L cDNA, *PPDK* cDNA, and 18S rDNA sequences using Primer Express 3.0. For each selected gene, three biological replicates were assayed independently. The qPCR amplifications were carried out in a total volume of 20 μL containing 10 μL of 2× SYBR Premix Ex TaqTM Ⅱ (TaKaRa Biotech Co., Dalian, China), 0.6 μL (10 μmol L^{-1}) of each primer, 2.0 μL of the diluted cDNA mix, and 6.8 μL de-ionized water. The qPCR amplification profile was obtained as follows: 95°C for 30 s followed by 40 cycles of 95°C for 5 s, 60°C for 10 s, and 72°C for 40 s. The $2^{-\Delta\Delta C_T}$ method was used to analyze the quantitative real-time PCR data.

1.7 Enzyme assays

The activity of RuBP carboxylase and PPDK in samples exposed to the treatments was measured, RuBP carboxylase activity by the method described by Gerard and Driscoll (1996) and PPDK activity by that described by Sayre, Kennedy and Pringnitz (1979) [33,34]; both methods were modified as required.

For measuring RuBP carboxylase activity, each sample was ground to a fine powder in liquid nitrogen and homogenized in pre-cooled rubisco extraction solution (1 mL g^{-1} fresh weight), pH 7.6, containing 40 mmol L^{-1} Tris-HCl buffer with 10 mmol L^{-1} $MgCl_2$, 0.25 mmol L^{-1} EDTA, and 5 mmol L^{-1} reduced glutathione. The homogenate was centrifuged at 10000×*g* for 10 min at 4°C. The activity was

Table 1 Primers used in the qPCR assay

Name		Primer sequence (5′–3′)
*rbc*L	F	TACAAATCTCAAGCCGAAACTG
	R	AATCTTTAGCAAATTGACCACG
PPDK	F	CACGAACGACCTTACGCAGA
	R	ACGGATCAAACGCCATCAC
18S rDNA	F	ATTAGATACCGTCGTAGTCTCAACC
	R	TCTGTCAATCCTTCCTATGTCTGG

measured in a 4.5 mL cuvette by adding 3 mL of a reaction mixture containing 0.2 mL NADH (5 mmol L^{-1}), 0.2 mL ATP (50 mmol L^{-1}), 0.1 mL enzyme extract, 0.2 mL creatine phosphate (50 mmol L^{-1}), 0.2 mL $NaHCO_3$ (0.2 mmol L^{-1}), 1.4 mL reaction buffer (0.1 mol L^{-1} Tris-HCl buffer, pH 7.8, with 12 mmol L^{-1} $MgCl_2$ and 0.4 mmol L^{-1} EDTA), 0.1 mL creatinephosphokinase (160 units mL^{-1}), 0.1 mL phosphoglycerate kinase (160 units mL^{-1}), 0.1 mL glyceraldehyde-3-phosphate dehydrogenase (160 units mL^{-1}), and 0.3 mL distilled water. The reaction was initiated by adding 0.1 mL ribulose-1, 5-bisphosphate (RuBP) to the reaction cuvette and *A* values were recorded every 20 s for 3 min by a spectrophotometer at 340 nm. The enzyme activity was expressed in terms of micromoles per gram of fresh weight per minute (μmol g^{-1} FW min^{-1}).

For measuring PPDK activity, the samples were ground to a fine powder in liquid nitrogen and homogenized in pre-cooled PPDK extraction solution at pH 8.3 (1 mL g^{-1} fresh weight) containing 100 mmol L^{-1} Tris-HCl buffer with 5 mmol L^{-1} mercaptoethanol and 2 mmol L^{-1} EDTA. The homogenate was centrifuged at 10000×*g* for 10 min at 4°C. The activity was measured in a 4.5 mL cuvette by adding 3 mL of a reaction mixture containing 0.1 mL Tris-HCl buffer (150 mmol L^{-1}, pH 8.3, with 18 mmol L^{-1} $MgSO_4$), 0.1 mL DTT (300 mmol L^{-1}), 0.1 mL PEP (30 mmol L^{-1}), 0.1 mL NADH (4.5 mmol L^{-1}), 0.1 mL AMP (30 mmol L^{-1}), 0.1 mL lactic dehydrogenase (60 units mL^{-1}), 0.1 mL enzyme extract, and 1.3 mL distilled water. The reaction was initiated by adding 0.1 mL pyrophosphate natrium to the reaction cuvette and the *A* values were recorded every 20 s for 3 min at 340 nm. The PPDK activity was also expressed in terms of micromoles per gram of fresh weight per minute (μmol g^{-1} FW min^{-1}).

2 Results

2.1 Transcriptome sequencing

To uncover the genomic mechanisms of *U. linza* when exposed to different forms of stress, a mixed transcriptome were sequenced by using Roche GS FLX Titanium as a platform to uncover the genomic mechanisms underlying rapid and successful colonization. A total of 503789 raw reads with an average length of 396 bp were generated by transcriptome sequencing, and 382884 reads were assembled into 13426 contigs with an average length of 1000 bases. KEGG analysis showed that 9356 reads were assigned to the carbon fixation pathway, which encode key genes of such enzymes as phosphoenolpyruvate carboxylase, aspartate aminotransferase, ribulose bisphosphate carboxylase, phosphoglycerate kinase, phosphoribulokinase, phosphoenolpyruvate carboxykinase, alanine transaminase, malate dehydrogenase (NADP+), pyruvate orthophosphate dikinase, and pyruvate kinase. This suggests the coexistence of the Calvin cycle (C_3) and Hatch-Slack (C_4) carbon fixation

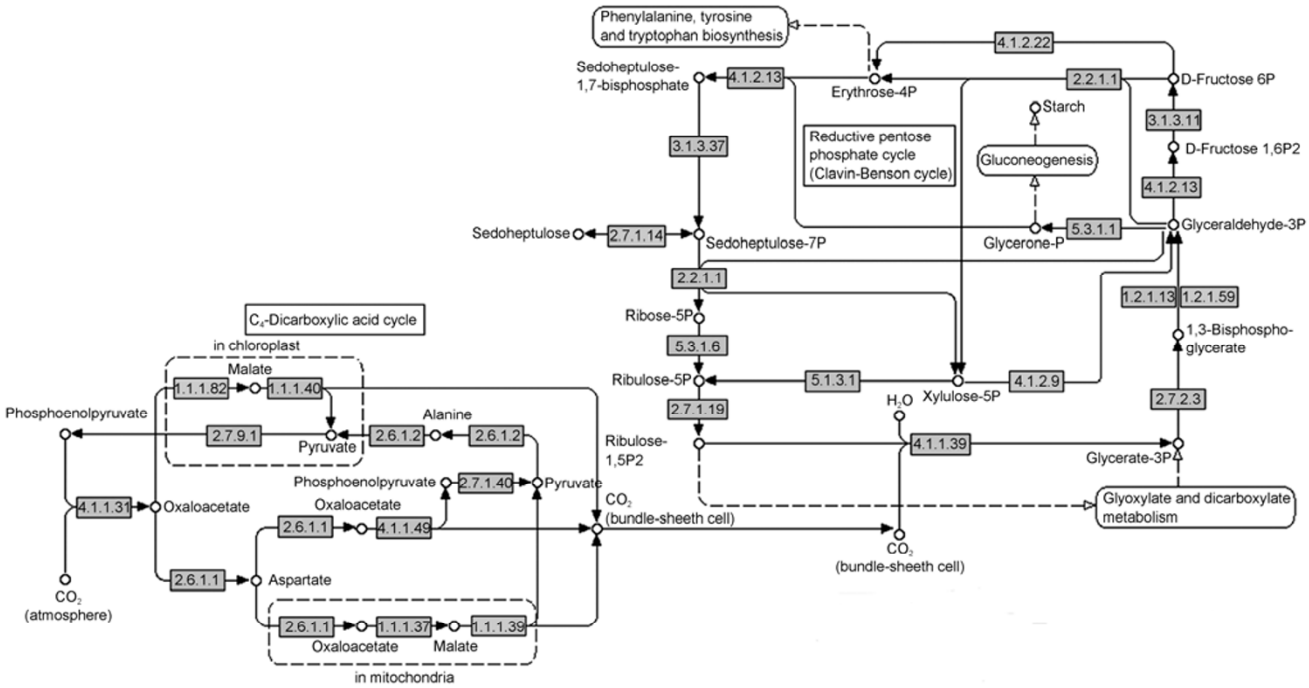

Figure 1 Carbon fixation pathway of *U. linza* from KEGG. EC numbers marked with light grey grounding indicate the key enzymes we got from transcriptome sequencing [28].

pathway in *U. linza* (Figure 1).

2.2 Photosynthetic parameters

The optimum quantum yield (F_v/F_m) and effective PSII quantum yield (Y(II)) were measured to investigate the growth condition in *U. linza* subjected to different forms and intensities of stress. As shown in Figure 2A, F_v/F_m and Y(II) reduced under desiccation conditions, which indicated desiccation was stress condition for *U. linza*. For the salinity and temperature experiment, F_v/F_m and Y(II) changed only slightly under high salinity, low salinity, high temperature and low temperature conditions (Figure 2B and D), which indicated that *U. linza* was not obviously stressed. Figure 2C shows F_v/F_m and Y(II) decreased quickly under high light intensity, which demonstrated high light intensity was stress condition for *U. linza*.

2.3 Analysis of *rbc*L and *PPDK* gene expression under various forms of stress

Expression levels of *rbc*L and *PPDK* genes under the different stress treatments were determined by relative quantitative PCR. Figure 3A and B shows the profile of expression of *rbc*L and *PPDK* as affected by desiccation for varying lengths of time. The expression levels of *rbc*L and *PPDK* under normal conditions were taken as 1. The transcript levels of *rbc*L reduced slowly along with the time whereas *PPDK* increased steadily at first, peaking (a 25.2-fold increase) at 4 h, and decreased thereafter. Levels of salinity affected the expression markedly compared to that under normal salinity (30‰), which was taken as 1. The transcript levels of *rbc*L decreased at both low and high levels of salinity, the highest expression being that at the normal level of 30‰, whereas those of *PPDK* exhibited the exact opposite, with higher levels at both low and high salinity (Figure 3C and D). Changes in expression levels under different light intensities are shown in Figure 3E and F. For each gene, the expression under 50 μmol m^{-2} s^{-1} was taken as 1. The expression level of *rbc*L in the dark was similar to that under normal light intensity, whereas that of *PPDK* was up-regulated 2-fold in the dark. Both peaked at 200 μmol m^{-2} s^{-1}. Although the expression of *PPDK* decreased under high light intensity, it was still higher than that under normal light intensity. Moreover, the effect of light intensities on *PPDK* was significantly higher than that on *rbc*L. The expression of *rbc*L and *PPDK* at normal temperature (10°C) was taken as 1, which happened to be the peak for both *rbc*L and *PPDK*; the levels of both fell at temperatures higher or lower than normal (Figure 3G and H) although *PPDK* was affected more significantly at 0°C and 30°C. In a word, the expression of *rbc*L was higher under normal conditions and lower under the adverse conditions, whereas that of *PPDK* was higher under some adverse con-

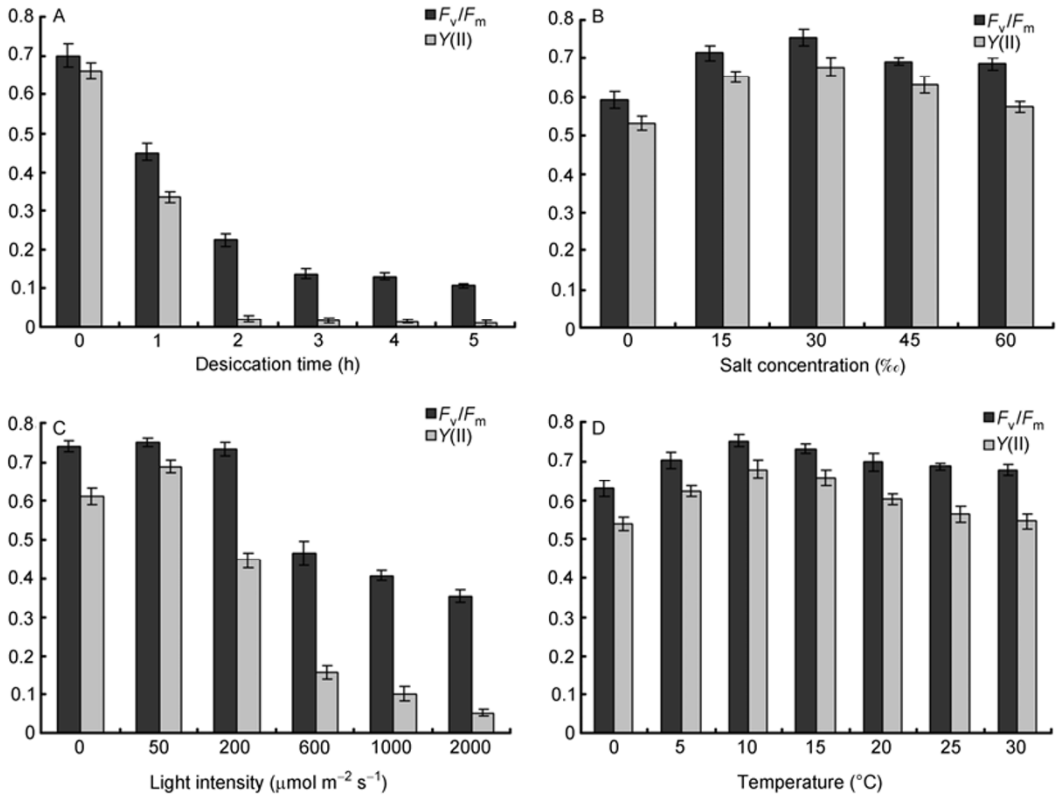

Figure 2 Optimum quantum yield (F_v/F_m) and effective PS II quantum yield (Y(II)) in *U. linza* under different forms and intensities of stress. A, Desiccation for different durations up to 5 h. B, Different salt concentrations for 1 h. C, Different light intensities for 1 h. D, Different temperatures for 1 h.

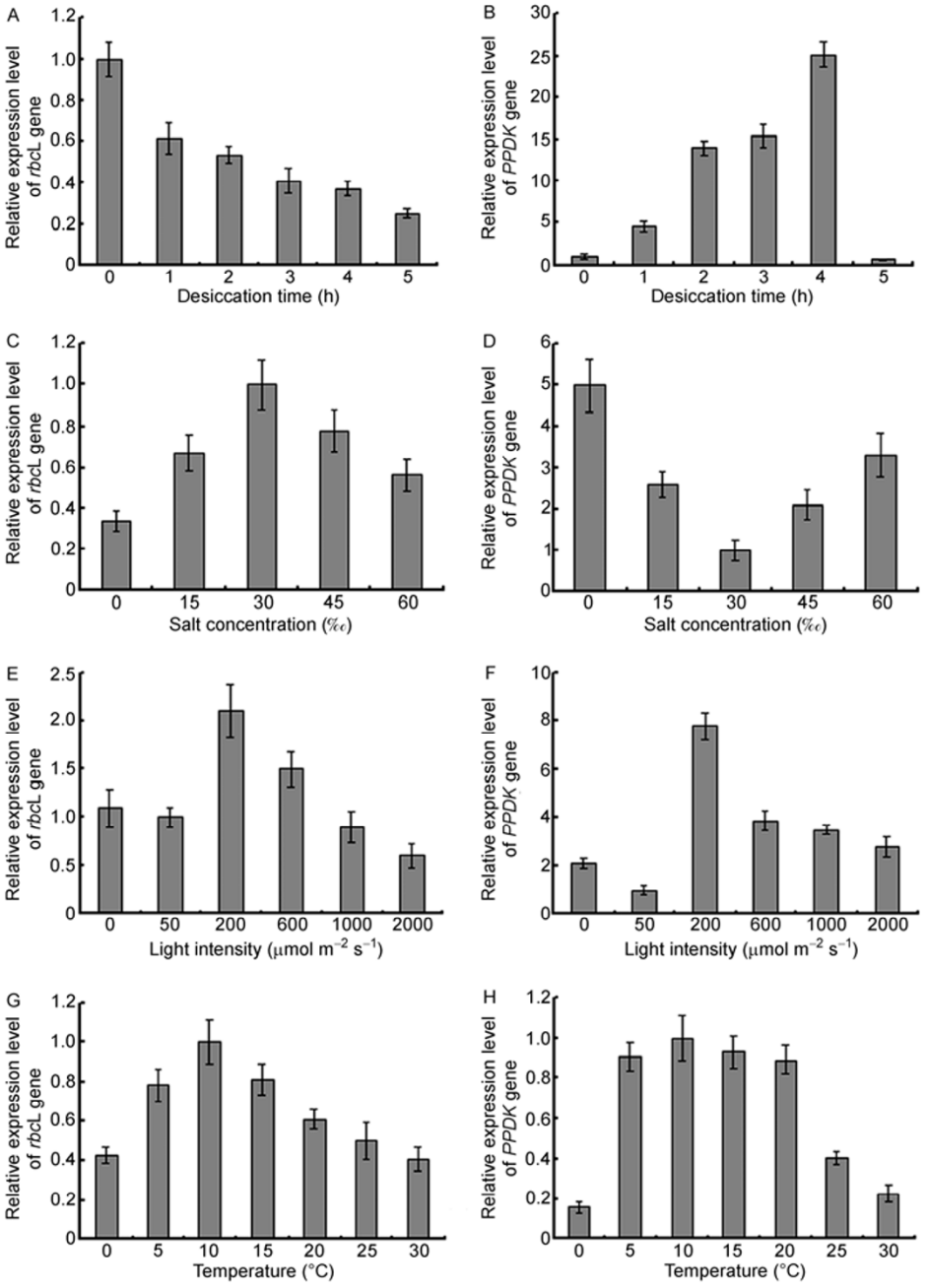

Figure 3 Real-time quantitative PCR analysis for the relative expression level of *rbc*L and *PPDK* gene in *U. linza* subjected to different forms and intensities of stress. Data are means of three independent experiments (±SD). Relative mRNA expression of *rbc*L and *PPDK* exposed to different stress conditions. A and B, Desiccation for different durations up to 5 h. C and D, Different salt concentrations for 1 h. E and F, Different light intensities for 1 h. G and H, Different temperatures for 1 h.

ditions, namely desiccation, high salinity, and low salinity.

2.4 Activity of RuBP carboxylase and PPDK

The activity of RuBP carboxylase weakend significantly with the duration of desiccation, the lowest level being nearly 50% of the normal level, whereas that of PPDK improved with the duration up to 4 h, the peak value being double the normal value, and decreased thereafter (Figure 4A). The activity of PPDK was very high under desiccation condition, even exceed RuBP carboxylase between 3–5 h. The effect of salinity level on RuBP carboxylase activity was the exact opposite of that on PPDK activity (Figure 4B): 30‰ salinity led to the highest level of RuBP carboxylase

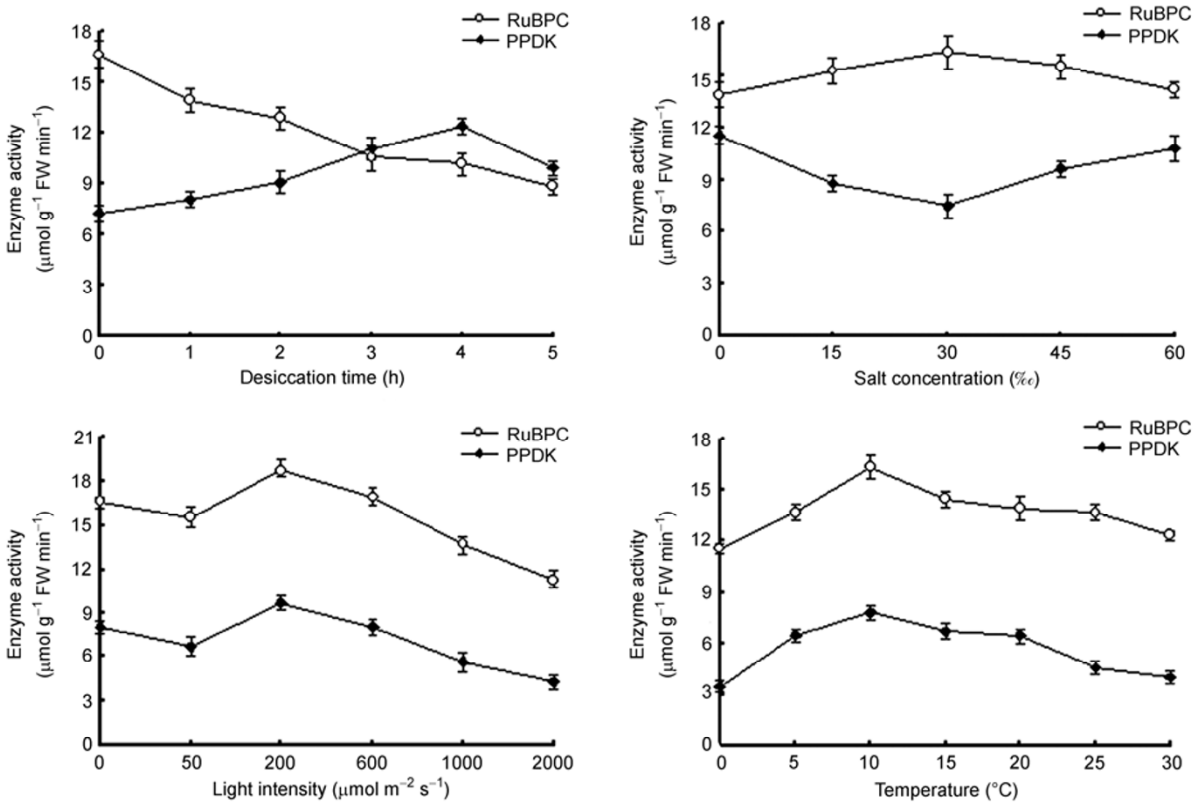

Figure 4 Activity of RuBP carboxylase and PPDK in *U. linza* exposed to different forms and intensities of stress. A, Desiccation for different durations up to 5 h. B, Different salt concentrations for 1 h. C, Different light intensities for 1 h. D, Different temperatures for 1 h.

activity and the lowest level of PPDK activity. Varying light intensities obviously influenced the activity of the two enzymes in a similar pattern: the activity began to rise initially, peaked at 200 μmol m^{-2} s^{-1}, and then dropped with light intensity strengthened further (Figure 4C). Almost no change in the activity of RuBP carboxylase and PPDK between the level under normal light intensity and darkness. Temperature affected both RuBP carboxylase and PPDK activity significantly and similarly (Figure 4D): both recorded maximum activity at 10°C, a level 1.4-fold and 2.2-fold than the lowest temperatures respectively. In short, both ribulose-1, 5-biphosphate carboxylase (RuBPCase) and PPDK were found to play a role in carbon fixation, with significantly higher PPDK activity across some stress conditions.

3 Discussion

The C_4 photosynthetic pathway is thought to be an exceptional evolutionary adaptation. Through a combination of structural and biochemical modifications brought about by mutation of genes encoding, for the most part, proteins involved in anaplerotic functions in ancestral C_3 species, C_4 plants gained the ability to outcompete these ancestors in arid, high light intensity, and saline environments that promote photorespiration [3]. C_4 plants are believed to have evolved gradually from C_3 plants through several intermediate stages of C_3-C_4 plants [35]. However, the evolutionary processes coming into being C_3-C_4 intermediates and C_4 plants are yet to be elaborated. In the present study, C_4 photosynthesis carbon fixation was found in the green-tide-forming macroalga *U. linza* by means of transcriptomic analysis and molecular determination, pointing to the existence and functioning of C_4 photosynthesis in *U. linza*. In addition, enzyme analysis indicated that PPDK was more important for plants under stress than for those growing under optimal growth conditions. These breakthroughs give new opportunities to further uncover the origins of the C_4 pathway and its functions in C_3 plants.

The expression levels of *PPDK* were higher than *rbc*L under some forms of stress. The transcript levels of *PPDK* increased under desiccation condition, whereas those of *rbc*L decreased. The activity of RuBP carboxylase and PPDK had similar tendency under desiccation condition, which indicated desiccation condition may induce the ex-

pression of C_4 photosynthesis and restrain the expression of C_3 photosynthesis. The expression level of *PPDK* rose at both low and high levels of salinity, whereas those of *rbc*L exhibited the exact opposite. The activity of RuBP carboxylase and PPDK also had similar tendency at high and low salinity conditions, which indicated high and low salinity conditions may induce the expression of C_4 photosynthesis and suppress the expression of C_3 photosynthesis. The expression of *rbc*L and *PPDK* had similar tendency under different light intensity and temperature conditions, which demonstrated high light intensity and high temperature may not induce C_4 photosynthesis in *U. linza*.

Recently, the C_4 pathway has been researched at the systems level by contrasting the transcriptome of a C_4 species to that of a closely related C_3 species [5,36]. Multiple independent origins of C_4 photosynthesis suggest that the evolution of a C_3 into a C_4 plants must have been relatively easy in genetic terms [37]. It is deduced that C_4 plants evolved from their C_3 ancestors at least 30 million years ago [38], and their expansion at the expense of C_3 plants in the late Miocene led to large-scale and lasting changes in climate and in ecosystems, modifying the frequency of fires and influencing the distribution and evolution of C_4 herbivores, including humans [1,39,40]. The C_4 photosynthetic pathway is one of the most significant complex adaptive traits ever acquired by hydrophytes, and the notion that aquatic environment is relatively 'benign' for plants and lacks the selection pressure that resulted in terrestrial C_4 CO_2-concentrating mechanism. Thus C_4 systems in algae appear to be ancient forms of C_4 photosynthesis that probably predate terrestrial C_4 plants and appear to have originated in waters subjected to localized CO_2 depletion [6].

Stress conditions often negatively affect key metabolic processes in plants [41]. However, enhanced activity of proteins related to the C_4 pathway, including PPDK, was found in higher plants under various abiotic forms of stress, such as drought, ozone, high salinity, the presence of heavy metals in soil, and the absence of phosphate and iron [40]. Moreover, the activity of these enzymes was enhanced in plants under biotic forms of stress caused by viral infections [40]. The functions of the enzymes of C_4 pathway appear to be more important for plants under stress conditions than for those under optimal growth conditions [42]. High temperature is a major environmental requirement for the evolution of C_4 pathway because high temperature directly stimulates photorespiration and dark respiration in C_3 plants [43,44]. The availability of CO_2 as a substrate also declines at high temperatures because of lower solubility of CO_2 relative to that of O_2 [45]. Aridity and salinity are also significant environmental elements because they promote stomatal closure and reduce the concentration of intercellular CO_2, which stimulate photorespiration and aggravate the deficiency of CO_2 as a substrate [46–48]. Many C_3-C_4 intermediates, such as intermediate species of *Heliotropium* [49], *Salsola* [50], *Alternanthera* [51], *Neurachne* [51], and a number of the *Flaveria* [52], are from arid or saline zones.

C_4 photosynthesis in marine environments is particularly significant because it is likely to influence the sensitivity of algae to changes in CO_2 concentrations [16]. If C_4 photosynthesis can account for a significant portion of carbon fixation in some marine species, it will affect various aspects of marine ecology and biogeochemistry [16]. *Ulva* species are also highly tolerant of variations in salinity, temperature, and irradiance and are considered to be the main cause of green tides. The existence and rise of C_4 photosynthesis expression level under some stress conditions in *U. linza* may account for the outbreaks of green tides and the high tolerance to various adverse environmental conditions shown by the species.

Although the exact mechanism of the uptake of inorganic carbon and its assimilation in marine green algae, particularly the relative importance of C_4 and C_3 photosynthesis under various conditions, need to be elucidated further, our results indicate that C_4 pathway may play a significant role in carbon fixation. Short-term photosynthetic ^{14}C labeling can be used to explore C_4 pathways in *U. linza* in greater detail. Intriguingly, the results point to the evolution of a photorespiratory CO_2-concentrating pump prior to the establishment of the C_4 pathway CO_2-concentrating pump [40]. This comprehensive study adds to our knowledge of C_4 evolution and provides adequate data to guide future work.

This work was supported by Shandong Science and Technology Plan Project (2011GHY11528), the Specialized Fund for the Basic Research Operating Expenses Program (20603022012004), National Natural Science Foundation of China (41176153), Natural Science Foundation of Shandong Province (2009ZRA02075), Qingdao Municipal Science and Technology Plan Project (11-3-1-5-hy), Qingdao Municipal Science and Technology Plan Project (10-3-4-11-1-jch), and National Marine Public Welfare Research Project (200805069).

1 Cerling T E, Wang Y, Quade J. Expansion of C_4 ecosystems as an indicator of global ecological change in the late Miocene. Nature, 1993, 361: 344–345
2 Christin P A, Freckleton R P, Osborne C P. Can phylogenetics identify C_4 origins and reversals? Trends Ecol Evol, 2010, 25: 403–409
3 Ludwig M. Carbonic anhydrase and the molecular evolution of C_4 photosynthesis. Plant Cell Environ, 2012, 35: 22–37
4 Whitney S M, Sharwood R E, Orr D, et al. Isoleucine 309 acts as a C_4 catalytic switch that increases ribulose-1,5-bisphosphate carboxylase/oxygenase (rubisco) carboxylation rate in *Flaveria*. Proc Natl Acad Sci USA, 2011, 108: 14688–14693
5 Gowik U, Westhoff P. The path from C_3 to C_4 photosynthesis. Plant Physiol, 2011, 155: 56–63
6 Bowes G. Single-cell C_4 photosynthesis in aquatic plants. In: Raghavendra A S, Sage R F, eds. C_4 Photosynthesis and Related CO_2 Concentrating Mechanisms. Dordrecht: Springer Science+Business

Media B.V., 2011. 63–80
7 Magnin N C, Cooley B C, Reiskind J B, et al. Regulation and localization of key enzymes during the induction of Kranz-less, C_4-type photosynthesis in *Hydrilla verticillata*. Plant Physiol, 1997, 115: 1681–1689
8 Spencer W E, Teeri J, Wetzel R G. Acclimation of photosynthetic phenotype to environmental heterogeneity. Ecology, 1994, 75: 301–314
9 Rao S K, Fukayama H, Reiskind J B, et al. Identification of C_4 responsive genes in the facultative C_4 plant *Hydrilla verticillata*. Photosynth Res, 2006, 88: 173–183
10 Beer S, Israel A, Drechsler Z, et al. Photosynthesis in *Ulva fasciata* V. Evidence for an inorganic carbon concentrating system, and ribulose-1,5-bisphosphate carboxylase/oxygenase CO_2 kinetics. Plant Physiol, 1990, 94: 1542–1546
11 Axelsson C, Larsson C, Ryberg H. Affinity, capacity and oxygen sensitivity of two different mechanisms for bicarbonate utilization in *Ulva lactuca* L. (Chlorophyta). Plant Cell Environ, 1999, 22: 969–978
12 Giordano M, Beardall J, Raven J A. CO_2 concentrating mechanisms in algae: mechanisms, environmental modulation, and evolution. Annu Rev Plant Biol, 2005, 56: 99–131
13 Reinfelder J R. Carbon concentrating mechanisms in eukaryotic marine phytoplankton. Annu Rev Mar Sci, 2011, 3: 291–315
14 Kremer B P. Aspects of carbon metabolism in marine macroalgae. Oceanogr Mar Biol Annu Rev, 1981, 19: 41–94
15 Reinfelder J R, Kraepiel A M I, Morel F M M. Unicellular C_4 photosynthesis in a marine diatom. Nature, 2000, 407: 996–999
16 Reinfelder J R, Milligan A J, Morel F M M. The role of the C_4 pathway in carbon accumulation and fixation in a marine diatom. Plant Physiol, 2004, 135: 2106–2111
17 Montsant A, Jabbari K, Maheswari U, et al. Comparative genomics of the pennate diatom *Phaeodactylum tricornutum*. Plant Physiol, 2005, 137: 500–513
18 Derelle E, Ferraz C, Rombauts S, et al. Genome analysis of the smallest free-living eukaryote *Ostreococcus tauri* unveils many unique features. Proc Natl Acad Sci USA, 2006, 103: 11647–11652
19 McGinn R J, Morel F M M. Expression and Inhibition of the carboxylating and decarboxylating enzymes in the photosynthetic C_4 pathway of marine diatoms. Plant Physiol, 2008, 146: 300–309
20 Beer S, Israel A. Photosynthesis of *Ulva* sp: III. O_2 effects, carboxylase activities, and the CO_2 incorporation pattern. Plant Physiol, 1986, 81: 937–938
21 Dong M, Zhang X, Zhuang Z, et al. Characterization of the LhcSR gene under light and temperature stress in the green alga *Ulva linza*. Plant Mol Biol Rep, 2011, doi: 10.1007/s11105-011-0311-8
22 Ye N, Zhang X, Mao Y, et al. 'Green tides' are overwhelming the coastline of our blue planet: taking the world's largest example. Ecol Res, 2011, 26: 477–485
23 Cohen R A, Fong P. Using opportunistic green macroalgae as indicators of nitrogen supply and sources to estuaries. Ecol Appl, 2006, 16: 1405–1420
24 Conley D J, Paerl H W, Howarth R W, et al. Controlling eutrophication: nitrogen and phosphorus. Science, 2009, 323: 1014–1015
25 Aquino R S, Grativol C, Mourao P A S. Rising from the sea: correlations between sulfated polysaccharides and salinity in plants. PLoS ONE, 2011, 6: e18862
26 Hatch M D. C_4 photosynthesis: a unique blend of modified biochemistry, anatomy and ultrastructure. Biochem Biophys Acta, 1987, 895: 81–106
27 Ishimaru K, Ohkawa Y, Ishige T, et al. Elevated pyruvate orthophosphate dikinase (PPDK) activity alters carbon metabolism in C_3 transgenic potatoes with a C_4 maize PPDK gene. Physiol Plantarum, 1998, 103: 340–346
28 Xu J, Fan X, Zhang X, et al. Evidence of coexistence of C_3 and C_4 photosynthetic pathways in a green-tide-forming alga, *Ulva prolifera*. PLoS ONE, 2012, 7: e37438
29 Huson D H, Auch A F, Qi J, et al. Megan analysis of metagenome data. Genome Res, 2007, 17: 377–386
30 Beer S, Larsson C, Poryan O, et al. Photosynthetic rates of *Ulva* (Chlorophyta) measured by pulse amplitude modulated (PAM) fluorometry. Eur J Phycol, 2000, 35: 69–74
31 Lin A P, Wang G C, Yang F, et al. Photosynthetic parameters of sexually different parts of *Porphyra katadai* var. *hemiphylla* (Bangiales, Rhodophyta) during dehydration and re-hydration. Planta, 2009, 229: 803–810
32 Dong M T, Zhang X W, Chi X Y, et al. The validity of a reference gene is highly dependent on the experimental conditions in green alga *Ulva linza*. Curr Genet, 2012, 58: 13–20
33 Gerard V A, Driscoll T. A spectrophotometric assay for RuBisCO activity: application to the kelp *Laminaria saccharina* and implications for radiometric assays. J Phycol, 1996, 32: 880–884
34 Sayre R T, Kennedy R A, Pringnitz D J. Photosynthetic enzyme activities and localization in *Mollugo verticillata* population differing on the leaves of C_3 and C_4 cycle operations. Plant Physiol, 1979, 64: 293–299
35 Ueno O. Structural and biochemical characterization of the C_3-C_4 intermediate *Brassica gravinae* and relatives, with particular reference to cellular distribution of Rubisco. J Exp Bot, 2011, 62: 5347–5355
36 Brautigam A, Kajala K, Wullenweber J, et al. An mRNA blueprint for C_4 photosynthesis derived from comparative transcriptomics of closely related C_3 and C_4 species. Plant Physiol, 2011, 155: 142–156
37 Westhoff P, Gowik U. Evolution of C_4 photosynthesis—looking for the master switch. Plant Physiol, 2010, 154: 598–601
38 Edwards E J, Osborne C P, Strömberg C A E, et al. The origins of C_4 grasslands: integrating evolutionary and ecosystem science. Science, 2010, 328: 587–591
39 Cowling S A, Jones C D, Cox P M. Consequences of the evolution of C_4 photosynthesis for surface energy and water exchange. J Geophys Res, 2007, 112: G01020
40 Gowik U, Brautigam A, Weber K L, et al. Evolution of C_4 photosynthesis in the genus *Flaveria*: How many and which genes does it take to make C_4? Plant Cell, 2011, 23: 2087–2105
41 Moons R, Valcke R, Montagu M V. Low-oxygen stress and water deficit induce cytosolic pyruvate orthophosphate dikinase (PPDK) expression in roots of rice, a C_3 plant. Plant J, 1998, 15: 89–98
42 Doubnerova V, Ryslava H. What can enzymes of C_4 photosynthesis do for C_3 plants under stress? Plant Sci, 2011, 180: 575–583
43 Brooks A, Farquhar G D. Effect of temperature on the CO_2/O_2 specificity of ribulose-1,5-bisphosphate carboxylase/oxygenase and the rate of respiration in the light. Planta, 1985, 165: 397–406
44 Sharkey T D. Estimating the rate of photorespiration in leaves. Physiol Plantarum, 1988, 73: 147–152
45 Jordan D B, Ogren W L. The CO_2/O_2 specificity of ribulose 1,5-bisphosphate carboxylase/oxygenase. Planta, 1984, 161: 308–313
46 Guy R D, Reid D M, Krouse H R. Shifts in carbon isotope ratios of two C_3 halophytes under natural and artificial conditions. Oecologia, 1980, 44: 241–247
47 Schulze E D, Hall A E. Stomatal responses, water loss and CO_2 assimilation rates of plants in contrasting environments. In: Lange O L, Nobel P S, Osmond C B, et al., eds. Physiological Plant Ecology II: Water Relations and Carbon Assimilation. Berlin: Springer-Verlag, 1982. 181–230
48 Adam P. Saltmarsh Ecology. Cambridge: Cambridge University Press, 1990
49 Frohlich M W. Systematics of Heliotropium section Orthistachys in

Mexico. Dissertation for Doctoral Degree. Boston: Harvard University, 1978
50 Voznesenskaya E V, Artyusheva E G, Franceschi V R, et al. Salsola arbusculiformis, a C_3-C_4 intermediate in Salsoleae (Chenopodiaceae). Ann Bot, 2001, 88: 337–348
51 Monson R K, Moore B D. On the significance of C_3-C_4 intermediate photosynthesis to the evolution of C_4 photosynthesis. Plant Cell Environ, 1989, 12: 689–699
52 Powell A M. Systematics of Flaveria (Flaveriinae-Asteraceae). Ann Mo Bot Gard, 1978, 65: 590–636